Mon. Not. R. Astron. Soc. **000**, 000–000 (0000) Printed 1 February 2008 (MN LATEX style file v1.4)

The properties of the peculiar Type Ia SN 1991bg. Analysis and discussion of two years of observations. ⋆

M. Turatto[1,2], S. Benetti[1], E. Cappellaro[2], I.J. Danziger[1,3], M. Della Valle[4], C. Gouiffes[5], P.A. Mazzali[3] and F. Patat[1,4]

[1] *European Southern Observatory, Karl-Schwarzschild-Strasse 2, D-8046 Garching bei München, Germany*
[2] *Osservatorio Astronomico di Padova, vicolo dell'Osservatorio 5, I-35122 Padova, Italy*
[3] *Osservatorio Astronomico di Trieste, via G.B. Tiepolo 11, I-34131 Trieste, Italy*
[4] *Dipartimento di Astronomia, Universitá di Padova, vicolo dell'Osservatorio 5, I-35122 Padova, Italy*
[5] *DAPNIA Sap/C.E. Saclay, F-91191, Gif sur Yvette Cedex, France*

Accepted ...Received ... ; in original form ....

ABSTRACT

Observations of the peculiar type Ia SN 1991bg in NGC 4374 collected at ESO–La Silla and Asiago are presented and discussed. The photometric coverage extends for 530 days and the spectroscopy for the first seven months after the explosion. The broad–band light curves in the early months have a narrower peak and a luminosity decline faster than other SNIa (14.6 and 11.7 $mag \times (100d)^{-1}$ in B and V respectively). The R and I light curves do not show the secondary peak typical of normal SNIa. The SN is intrinsically very red ($(B-V)_{max} = 0.74$) and faint ($B_{max} = -16.54$). The light curves flatten with age but remain significantly steeper (2.0 and 2.7 $mag \times (100d)^{-1}$ in B and V between 70 and 200 day) than the average. Consequently the *uvoir* bolometric light curve of SN 1991bg is fainter with a steeper decline than that of the normal SNIa (e.g. 1992A). This object enhances the correlation which exists between the peak luminosity of SNIa, the decline rate and the kinetic energy.

Peculiarities are evident in the spectra at various phases. The continuum at maximum is very red and the photospheric expansion velocity extremely low. There are a number of unusual spectral features, in particular a broad absorption between 4200 and 4500 Å which is attributed to TiII and the appearance, as early as one month after maximum, of nebular emission of possibly [CoIII] $\lambda 5890 - 5908$. Nevertheless, contrary to previous claims (Ruiz-Lapuente et al 1993), the spectral evolution retains a general resemblance to that of other SNIa until the latest available observation (day 203). At this epoch one sees the typical emission features of SNIa at late times although they are significantly narrower (FWHM$\sim$ 2300 km s^{-1}). This facilitates the identification of most lines with forbidden emission of [FeII], [FeIII] and [CoIII]. The emission feature centered at about $\lambda 6590$ is difficult to reconcile with the previous identification as Hα, unless asymmetries in the ejecta or ad hoc binary configurations are invoked.

This work suggests that the explosion energy was probably a factor 3 to 5 lower than in normal SNIa. Whether this resulted from an explosion of a sub–Chandrasekhar mass WD is not unambiguously established.

Key words: supernovae: general – supernovae: individual: 1991bg, 1992A, 1986G, 1981B. 1992K, 1991T, 1989B, 1994D, 1991F – supernova remnants.

1 INTRODUCTION

Supernovae of type Ia have been considered for decades and are still considered by some to be almost perfect distance indicators. Actually, some scatter in their photometric proper-

⋆ Based on observations collected at ESO-La Silla (Chile) and Asiago (Italy).

ties was suggested as early as the late sixties (Pskovskii 1967; Pskovskii 1971; Barbon et al. 1973), but it has been mostly attributed to photometric errors (e.g. Sandage & Tammann 1993).

However, in recent years the discovery of two extreme SNIa, 1991T and 1991bg, challenged the standard candle scenario for SNIa, 1991T being brighter than the average SNIa (Ruiz-Lapuente et al. 1992; Phillips et al. 1992; Mazzali et al. 1995) and 1991bg significantly fainter (Filippenko et al. 1992; Leibundgut et al. 1993). The two SNe also showed distinctive spectral peculiarities which, however, might have gone unnoticed if only sparse observations had been gathered. Therefore, a question arises: are the samples of SNIa used as standard candles heavily contaminated by such extreme objects and how much such contamination affects the derived values of H_0 and q_o? The question has been further complicated by the recognition that even SNIa with very similar spectra can show a significant spread in absolute magnitude (Patat et al. 1996), which may correlate with the photometric evolution and even with the morphological type of the parent galaxy (Hamuy et al. 1995).

Supernovae of different intrinsic brightness have different probabilities of being detected, hence it is expected that the intrinsic fraction of faint SNe is higher than the actual percentage of discoveries. This has implications for the chemical evolution of the galaxies, since SNIa are thought to be a primary source of Fe-peak elements.

The goal of this paper is to present and discuss new photometric and spectroscopic observations of SN 1991bg describing the evolution of this object until the late nebular stages and to highlight peculiarities and similarities compared with other SNIa. Some quantitative indications on the precursor star and the total amount of synthesized material will also be given.

2 OBSERVATIONS AND REDUCTIONS

2.1 Photometry

SN 1991bg was discovered on 1991 Dec. 9.8 by R. Kushida (Kosai et al. 1991) about 1 arcmin South of the nucleus of the elliptical galaxy NGC 4374, which is located near the center of the Virgo cluster.

The observations at the ESO–La Silla and Asiago Observatories started soon after the discovery and continued for the next seven months, until the Virgo cluster disappeared behind the Sun. Eventually the SN was detected 530 days after maximum.

The broad band B, V and R photometry (together with two I-band observations) are listed in Tab. 1. Depending on the brightness of the object and on instrument schedule, several different telescopes were used. On photometric nights sequences of standard stars (Landolt 1992) were observed which allowed the determination of the color equations of the photometric systems. These were in good agreement with the determinations by other authors. For calibrating the non–photometric nights, a local sequence was established around the galaxy. For the stars in common with the sequence of Leibundgut et al. (1993) and Filippenko et al. (1992), our measurements agree to within a few hundredths of a magnitude with those of the above authors.

Until 200d the photometric measurements were performed with the ROMAFOT package, whose utilization in the context of SNe has already been discussed (cfr. Turatto et al. 1993). The errors in the SN magnitudes depend on the contrast of the star against the galaxy background and were estimated to range from 0.05 at early epochs up to 0.2 mag at seven months. In Fig. 1 our measurements are plotted together with those by Filippenko et al. (1992) and Leibundgut et al. (1993). It is evident that while at early epochs the agreement between the different sources is good, it becomes poor as the SN fades. In particular, at about 150 days our estimates appears 0.5 mag fainter than those of Leibundgut et al. (1993). Since the zero point is the same (the local sequences coincide), the inconsistency has to be attributed to the measuring technique. Both Leibundgut et al. and Filippenko et al. derived the SN magnitudes by means of aperture photometry but, while the former authors measured the background in an annulus around the SN, the latter ones, exploiting the symmetric surface brightness profile of the elliptical parent galaxy, subtracted the image of the galaxy rotated by 180° around the major axis. We have tested the measurements of the SN magnitude with both these methods: already at epochs earlier than < 100 days the subtraction of annuli produced results dependent on the radii of the annuli, while the subtraction of the rotated galaxy gave results within a few hundredths of magnitude of our ROMAFOT determination.

Based on the first, unsuccessful attempt to recover the SN, in January 1993, upper limits for the SN magnitude were derived by placing increasingly fainter artificial stars at the precise position of the SN relative to nearby stars. The result was $V \geq 22.5$ and $R \geq 22.1$. A somewhat fainter upper limit was obtained using an image taken with the WFC of HST on 6 March, 1993 in the F555W passband (very close to the standard V) and retrieved from the HST Archive. The exposure was not very deep (300 s) and the frame was processed with the Routine Science Data Processing pipeline. Using both the internal calibration of the frame and a faint comparison sequence calibrated with our deep ground–based observations, we found V$\geq$ 23.5 for the SN at this epoch.

Finally, a series of 17 exposures (total observing time 170 min) was obtained on May 26, 1993, i.e. 530 days after B maximum. The frames were flat fielded, aligned and co-added into a single exposure in order to improve the signal-to-noise ratio. Although the seeing was not exceptional (1.15 arcsec) a stellar image was found within 0.1 arcsec from the expected position (Fig 2). In this case, the SN magnitude was also measured using SNOOPY, a new software especially designed for SN photometry by one of us (F.P.). As for ROMAFOT, in SNOOPY the magnitude is derived by means of the point-spread-function-fitting technique, but background fitting was improved and interactivity enhanced (Patat, in preparation). The resulting magnitude was V=24.95. The error of the measurement was estimated by means of artificial star tests. The dispersion of the recovered magnitudes of 50 artificial stars positioned near the SN was r.m.s.=0.40 mag.

2.2 Spectroscopy

The journal of the spectroscopic observations is given in Tab. 2, where the instrumentation and the spectral ranges

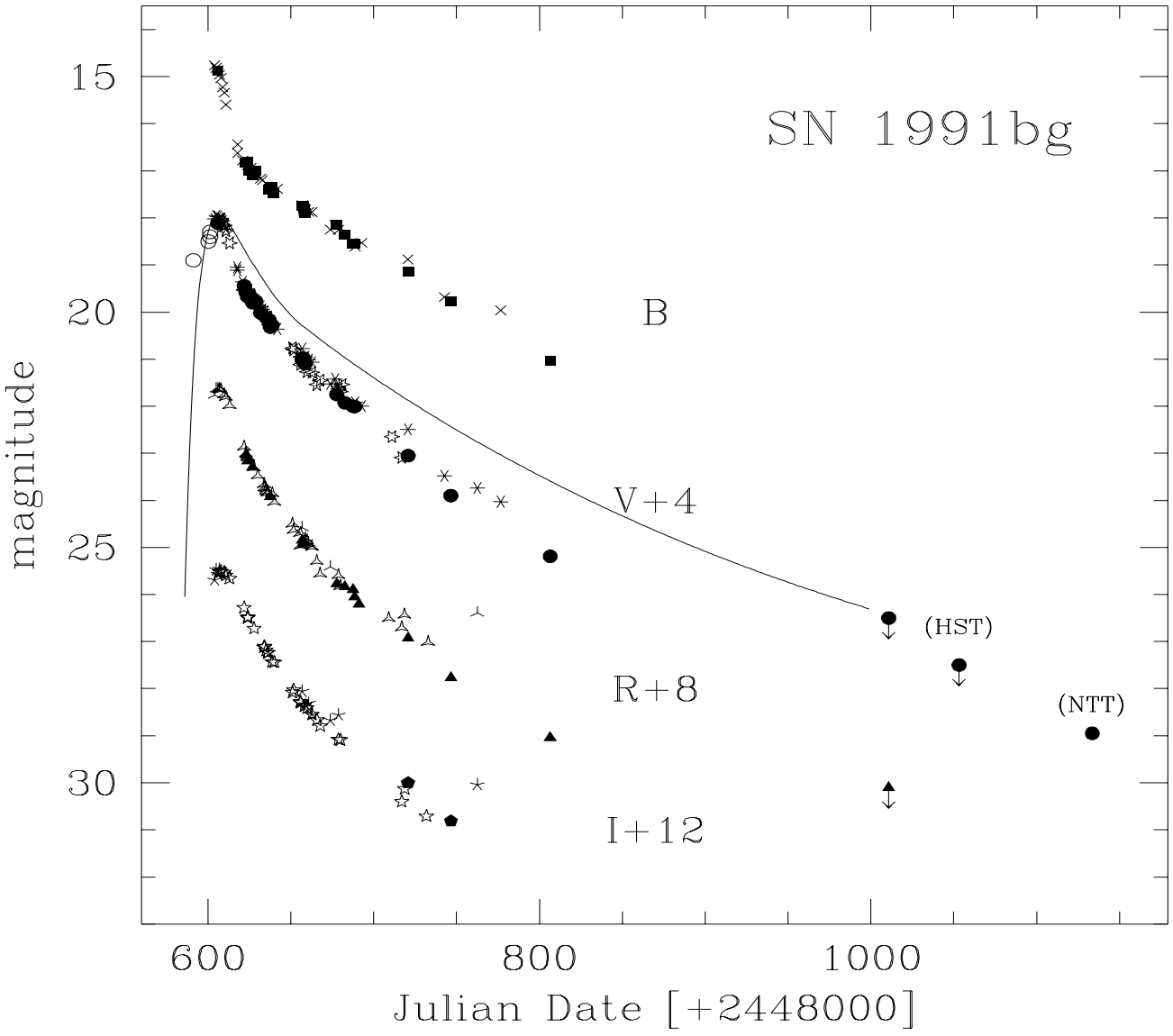

Figure 1. The light curves of SN 1991bg in the BVRI bands. Ordinates are B magnitudes while all others bands have been shifted down as indicated. The solid line is the V light curve of SN 1992A (Wheeler & Benetti 1995) adjusted to match the V maximum of 1991bg. Filled symbols are the observations presented here, starred symbols are from Filippenko et al. (1992), skeletal symbols are from Leibundgut et al. (1993) and open symbols from IAU Circulars.

are indicated. The spectra were calibrated in wavelength with adjacent spectra of comparison lamps and flux calibrated with spectrophotometric standard stars observed in the same nights. Different exposures obtained during the same night (or in consecutive nights at late epochs) with the same configuration have been co-added in order to increase the signal–to–noise ratio while those obtained with different gratings or grisms have been merged. When the SN broad-band photometry was available on the same night, the absolute flux calibrations of the spectra were checked. In most cases corrections were not needed, but if necessary, corrections of the order of few tenths of a magnitude were applied.

During the observations particular care was given to the accurate positioning of the slit, whose width was typically between 1.5 and 2 arcsecs. When the spectra were obtained at large zenith distances the slit was aligned along the parallactic angle, otherwise a second exposure was taken with a wider slit (5–10 arcsecs) in order to ensure that all the light from the object entered the slit. The spectral resolution was typically 10Å at the NTT, 12Å at the 2.2m telescope, 20Å at the 3.6m and 22Å at the 1.8m. Composite

Table 1. CCD photometry of SN 1991bg

Date	JD[a]	B	V	R	I	Instr.
15/12/91	8605.85	14.87	14.11			NTT
31/12/91	8621.92		15.44			NTT
01/01/92	8622.84	16.82	15.57	15.04		0.9m
02/01/92	8623.84	16.81	15.62	15.16		0.9m
02/01/92	8623.85		15.67			NTT
03/01/92	8624.84	16.99	15.63	15.14		0.9m
05/01/92	8626.84	17.10	15.80	15.30		0.9m
07/01/92	8628.85	17.00	15.77			0.9m
10/01/92	8631.85		16.02			0.9m
15/01/92	8636.67	17.40	16.16			NTT
16/01/92	8637.67	17.38	16.32	15.92		NTT
17/01/92	8638.70	17.34	16.28			NTT
18/01/92	8639.60	17.47				NTT
04/02/92	8656.86	17.75	17.01	16.85		3.6m
05/02/92	8657.61	17.75	16.98	16.94		1.8m
05/02/92	8657.88	17.81	17.03	16.88		3.6m
06/02/92	8658.53	17.90	17.10	16.90		1.8m
25/02/92	8677.67	18.15	17.75	17.77		NTT
01/03/92	8682.75	18.35	17.93	17.84		2.2m
06/03/92	8687.55	18.55	18.00	17.90		1.8m
07/03/92	8688.54	18.55	18.01	18.05		1.8m
10/03/92	8691.50			18.20		NTT
08/04/92	8720.75	19.14	19.05	18.93	18.00	2.2m
04/05/92	8746.60	19.78	19.90	19.77	18.81	3.6m
03/07/92	8806.52	21.03	21.19	21.04		3.6m
23/01/93	9010.81		> 22.50	> 22.10		3.6m
06/03/93	9053.24		> 23.50			HST
26/05/93	9133.57		24.95			NTT

a) +2440000
NTT=New Technology Telescope+EMMI,
3.6m=ESO 3.6m+EFOSC,
2.2m=ESO/MPI 2.2m+EFOSC2,
1.8m=Asiago 1.8m+CCD camera,
0.9m=Dutch 0.9m+CCD camera,
HST=HST+WFC+F555W

spectra obtained by merging data from different equipment or configurations (e.g. grisms or gratings) may thus have different resolutions at different wavelengths. For instance, the spectrum at t=+117 d, has a resolution of about 12Å between 4470 and 8420Å and about 30Å outside this range (cfr. Fig 6).

3 LIGHT CURVES

The light curves of SN 1991bg in the first months after maximum, already discussed by Filippenko et al. (1992) and Leibundgut et al. (1993), are updated in Fig. 1 with the inclusion of our new data. It is confirmed that the photometric evolution of SN 1991bg differs from that of normal SNIa: the maximum peak is narrower and the luminosity decline faster. Premaximum observations are scanty and quite uncertain, therefore little can be said about the rise to maximum light. Our best estimates of the epochs and magnitudes at maximum are reported in Tab. 3 and are in good agreement with previous estimates.

The light curves of SN 1991bg in the first 2 months after maximum are compared in Fig. 3 to those of the normal SNIa 1994D and of the somewhat peculiar SNIa 1986G. The general behavior of SNIa, showing a slower luminosity decline in the red than in the blue, holds also for SN 1991bg which however shows the steepest initial luminosity decline rate, namely 14.6 and 11.7 $mag \times (100d)^{-1}$ in B and V respectively, to be compared with 12.5 and 7.2 $mag \times (100d)^{-1}$ measured in SN 1994D (Patat et al. 1996). The secondary maximum, which is quite pronounced in the I light curve of SN 1994D, is absent in SN 1991bg.

The light curve evolution of SN 1986G is also faster than that of SN 1994D (12.8 and 8.6 $mag \times (100d)^{-1}$ in B and V respectively) albeit not as fast as SN 1991bg (cfr. Fig. 3). Unfortunately the R and I light curves of SN 1986G are not available, and so a comparison with SN 1991bg, which departs strongly from the standard SNe Ia in these bands, is not possible but neither SN shows the secondary maxima in the near–IR typical of normal SNIa (Frogel et al. 1987; Porter et al. 1992).

As early as 15 days after maximum, the B light curve of SN 1991bg begins a slower decline, while at increasingly redder wavelengths the change of slope occurs later and is less evident. Therefore, the value of $\Delta(m)_1$ given in Tab. 3 for the B band corresponds to the parameter $\delta m_{15}(B)$ defined by Phillips (1993). Our determination is in good agreement

Table 2. Journal of the spectroscopic observations of SN 1991bg

Date	phase[a] (days)	JD[b]	Wavelength range (Å)	Instrum.
14/12/91	0.7	8604.65	3650-9250	1.8m
15/12/91	1.6	8605.60	4030-9200	1.8m
15/12/91	1.9	8605.85	3880-8120	NTT
29/12/91	15.6	8619.57	4170-8450	1.8m
31/12/91	17.9	8621.88	4170-9800	NTT
02/01/92	19.5	8623.85	4170-7860	NTT
14/01/92	31.5	8635.54	3850-9420	1.8m
15/01/92	32.5	8636.54	6850-11000	1.8m
16/01/92	33.7	8637.67	4160-7950	NTT
28/01/92	45.6	8649.56	3560-9040	1.8m
01/02/92	49.8	8653.83	3560-7100	2.2m
04/02/92	52.7	8656.65	3560-9200	1.8m
04/02/92	52.9	8656.87	3600-6720	3.6m
13/02/92	61.6	8665.56	4050-8410	1.8m
25/02/92	73.7	8677.67	5400-6500	NTT
01/03/92	78.8	8682.79	4470-8200	2.2m
10/03/92	87.5	8691.50	4200-10000	NTT
08/04/92	116.7	8720.71	3560-9100	2.2m
04/05/92	142.6	8746.60	3730-6900	3.6m
03/07/92	202.5	8806.52	3770-6900	3.6m

a) from B maximum (J.D. 2448604.0)
b) +2440000
NTT=New Technology Telescope+EMMI,
3.6m=ESO 3.6m+EFOSC,
2.2m=ESO/MPI 2.2m+EFOSC2,
1.8m=Asiago 1.8m+B&C

with his estimate even after the inclusion of our new photometry.

3.1 The photometric evolution

Previous analyses have shown that the light curve of SN 1991bg can be well approximated by 3 segments spanning from day 4 to 20, 20 to 60 and 60 to 200, respectively. The inclusion of our new data changes the positions of the bending points slightly with respect to earlier determinations (Filippenko et al. 1992; Leibundgut et al. 1993). The epochs of the bending points and the slopes (in units of $mag \times (100d)^{-1}$) of the three segments are given in Tab. 3. As we will argue later, the fast evolution of the early light curve are indicative of a small ejecta mass.

The new observations of Tab. 1 are especially important since they constrain the late time photometric behavior of SN 1991bg. Two months after maximum, the second bending point in the light curves marks the beginning of the radioactive tail which then remains linear until at least day 200 (Tab. 3). Again the luminosity decline rate of SN 1991bg in this phase is significantly faster than those of all other well-observed SNIa, which typically have a rate of 1.5 $mag \times (100d)^{-1}$ (cfr. Turatto et al. 1990, Suntzeff 1995).

Finally, the observation 530 days after maximum indicates that after day 200 the luminosity decline was significantly slower, 1.2 $mag \times (100d)^{-1}$ based only on the two last observations. Due to the 300 day gap in the observations, it is impossible to determine if the change was gradual or if a new bending point characterizes the late light curve. We note, however, that the observed decline rate is still steeper than that of ^{56}Co to ^{56}Fe decay (0.98 $mag \times (100d)^{-1}$).

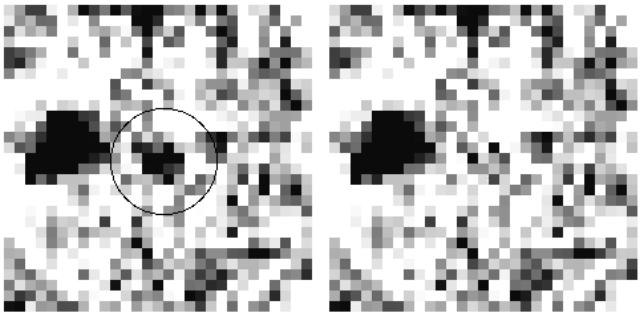

Figure 2. Co-added V image of SN 1991bg in NGC 4374 obtained on May 26, 1993 (i.e. 530 days after maximum) at the NTT (+EMMI) (total exposure 170 min, seeing 1.15 arcsecs). The left panel shows the co-added original frame once the smooth background of the parent galaxy has been subtracted ($\mu_V \sim 21.4$ mag/arcsec^{-2}). The expected position of the SN has been encircled. The right panel shows the same area after the subtraction of the SN.

3.2 The absolute magnitude at maximum

NGC 4374, the parent galaxy of SN 1991bg, lies in the core of the Virgo cluster. This makes it possible to compare directly the apparent magnitude of SN 1991bg with that of other SNIa in the cluster. A list of the Virgo SNIa with "normal" spectra and reliable photometry was given by Patat et al. (1996) (their Tab. 4): the average apparent magnitude is $B_{max} = 12.22 \pm 0.44$, to be compared with $B_{max} \sim 14.75$ for SN 1991bg. Two other SNIa have been discovered in NGC 4374, SN 1957B and 1980I (cfr. Turatto et al. 1994). Both SNe show apparent magnitudes in agreement with that of normal SNIa in Virgo. Therefore, if no significant reddening was present, SN 1991bg was at maximum 2.5 magnitudes fainter in the B band than normal SNIa.

Strong reddening is not expected, since the parent galaxy is elliptical. Actually a dust lane, elongated in the E–W direction, crosses the galaxy nucleus (cfr. Filippenko

Table 3. Basic photometric data of SN 1991bg

	B	V	R	I	bol
			MAXIMA		
J.D.(+2448000)	~ 604.0	605.5 ± 1.0	606.0 ± 1.0	608.0 ± 1.0	605.0 ± 1.0
mag.	$\sim 14.75 \pm 0.1$	13.96 ± 0.05	13.63 ± 0.05	13.50 ± 0.05	
abs.mag*	-16.54 ± 0.32	-17.28 ± 0.31	-17.58 ± 0.31	-17.68 ± 0.31	-16.50 ± 0.34
$\log L$ [erg s^{-1}]					42.20 ± 0.14
		FADING RATES $[mag \times (100d)^{-1}]$ (phase range [days])			
early	14.6(3-14)	11.7(6-14)	9.4(6-24)	7.3(9-24)	9.1(4-20)
intermediate	2.6(17-59)	4.2(17-64)	4.6(30-59)	4.8(30-64)	3.6(30-70)
late	2.0(70-203)	2.7(70-203)	2.6(70-203)	2.7(75-143)	2.6(70-203)
very late		1.2(203-530)			
		BENDING POINTS			
epoch$_1$ [days]	15	17	24	28	22
$\Delta(m)_1$ [mag]	1.95	1.44	1.77	1.50	1.70
epoch$_2$ [days]	60	60	68	65	70
$\Delta(m)_2$ [mag]	3.25	3.34	3.87	3.30	3.50

COLORS	$(B-V)$	$(V-R)$	$(V-I)$
day 0 (B max.)	0.74	0.25	0.33
day 15–17	1.45	0.60	1.25

(*) $E(B-V) = 0.05$, $\mu = 31.09$

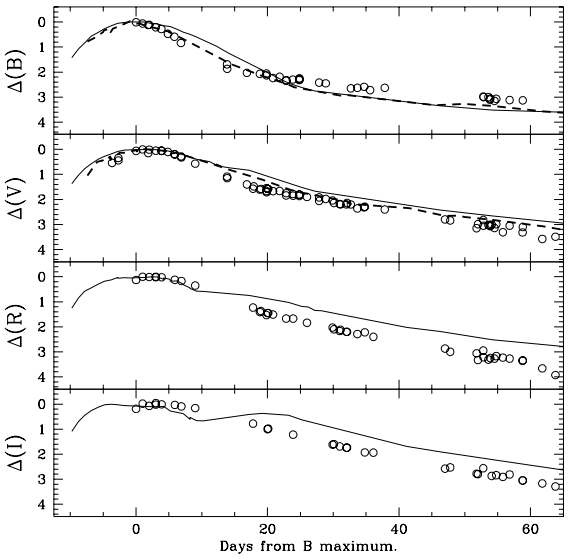

Figure 3. Comparison between the early light curves of SN 1991bg (symbols), SN 1994D (solid lines, Patat et al. 1994) and SN 1986G (short dashed line, Cristiani et al. 1992). In the four panels, zero in the abscissa corresponds the epoch of the B maximum while in the ordinates it is the magnitude at maximum in the specific photometric band.

et al. 1992, Leibundgut et al. 1993) but the SN is located about 1 arcmin to the south of the nucleus and hence no significant contamination is expected. In fact, a careful examination of our best S/N spectra (cfr. Sect. 4) did not show signs of narrow interstellar NaI D at the expected position (5913Å). In a few spectra a weak absorption might be present at about 5890 Å that can be due to interstellar NaI D within the Galaxy ($A_B = 0.13$, Burstein & Heiles 1984). Indirect, but independent, support for low reddening comes from the spectral modeling at early and late epochs by Mazzali et al. (1996). Those models require low photospheric temperatures. This, together with the fact that all 3 colours, $B-V$, $V-I$, $V-R$ are redder than normal SN Ia immediately after maximum but return to normal colours 30 days past maximum, suggests that neither internal dust formation nor line blanketing due to additional abnormally strong lines are the cause of the red colours. In agreement with other papers on this SN, we will adopt in the following E(B-V)$\sim 0.05 \pm 0.02$ as the total reddening suffered by SN 1991bg. Given the low reddening, it is clear that SN 1991bg was *intrinsically* faint and red.

For homogeneity with Patat et al. 1995 and Vaughan et al. (1995) who studied large samples of SNIa, we adopt for NGC 4374 the distance derived using the SBF method ($\mu = 31.09 \pm 0.30$, Ciardullo et al. 1993). Taking into account the (small) reddening, we obtain for SN 1991bg the following absolute magnitudes: $M_{\rm B} = -16.54 \pm 0.32$, $M_{\rm V} = -17.28 \pm 0.31$, $M_{\rm R} = -17.58 \pm 0.31$ and $M_{\rm I} = -17.68 \pm 0.31$. These values are significantly fainter and redder than the mean, $M_{\rm B} = -18.64 \pm 0.05 + 5log(H_o/85)$ and $M_{\rm V} = -18.63 \pm 0.06 + 5log(H_o/85)$, found by Vaughan et al. (1995) for their

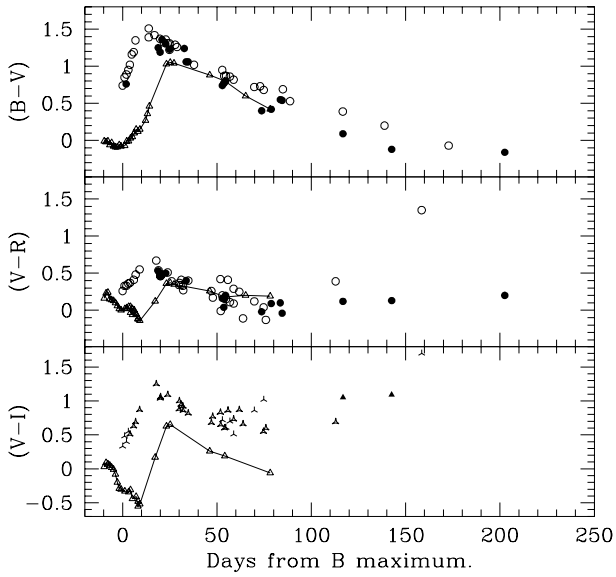

Figure 4. The color curves of SN 1991bg compared to those of SN 1994D (connected by solid lines) which has a reddening similar to SN 1991bg (Patat et al. 1995). Filled symbols are observations from Table 1, open symbols are data from literature. Note the scatter at late epochs.

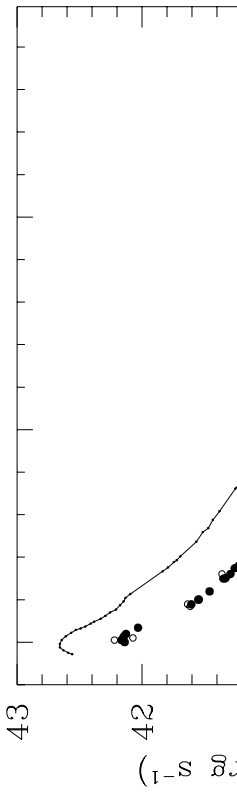

Figure 5. Bolometric light curves of SNe 1991bg (symbols) and 1992A (line). Filled symbols refer to BVRI photometry from this paper and ¿from literature while open symbols are derived from the flux calibrated spectra of Table 2 with wide wavelength range. For the computation of the last point (day +203) the I photometry has been linearly extrapolated form the previous epochs. For SN 1991bg we have used a bolometric correction of 0.1 dex constant with time (see text for a discussion of the relative luminosity), distance modulus 31.09 and reddening correction E(B-V)=0.05. The data for SN 1992A are from Suntzeff (1995).

ridge–line SNIa, i.e. SNIa which suffered little extinction. SN 1991bg is even more so compared to the average SNIa magnitudes derived with the Cepheid distance calibration ($M_{\rm B}= -19.65 \pm 0.13$ and $M_{\rm V}= -19.60 \pm 0.11$, Saha et al. 1995).

At present, it is widely accepted that some degree of heterogeneity is present within the class of SNIa (e.g. Patat et al. 1995, Hamuy et al. 1995). This may be partially described by a relation between the peak luminosity and the initial decline rate (Pskovskii 1967; Phillips 1993; Hamuy et al. 1995). However, even in this context the low luminosity of SN 1991bg is exceptional, since this SN does not lie on the extension of the peak luminosity–decline rate relation observed for the slowly declining objects (Hamuy et al. 1995).

3.3 Color curves

The evolution in three different colors is shown in Fig. 4 in which the comparison is made with the well-studied SN 1994D which had comparable reddening to 1991bg and whose color evolution was similar to 1992A (Patat et al. 1996).

The two SNe show significantly different color evolutions. At maximum, SN 1991bg had $(B-V) \sim$ 0.75, i.e. it was $\sim$ 0.8 mag redder than SN 1994D. Were the color differences due to reddening for SN 1991bg, which we excluded (cfr Sect. 3.2), this would indicate $A_B = 3.2$ yielding $M_{\rm B}= -19.54$. With such values SN 1991bg would be the brightest SNIa in the samples studied by Vaughan et al. (1995) and Phillips (1993). At the time of maximum, SN 1994D was still evolving to the blue, with minima in $(V-R)$ and $(V-I)$ corresponding to the minima between the two peaks of the R and I light curves (Patat et al. 1996). On the contrary, SN 1991bg at the same epoch was already rapidly evolving to the red. SN 1991bg reached the reddest colors $(B-V)$=1.45, $(V-R)$=0.60 and $(V-I)$=1.25) at about t=15-17d, corresponding to the first bending point of the B light curve, while in SN 1994D the maxima of the colors were reached somewhat later (t=25d) at $(B-V)$=1.05, $(V-R)$=0.37 and $(V-I)$=0.65. Diversity in the color evolution of SNIa (especially in proximity of maximum) have been noted by Maza et al. (1994) and Patat et al. (1996) but, to our knowledge, no other object appears as odd as SN 1991bg.

After the color maxima, SN 1991bg turned to the blue and starting about day 40-50 it matched the $(B-V)$ and $(V-R)$ curves of normal SNIa (Fig 4). The $(V-I)$ curve, instead, never conformed with that of 1994D, remaining always considerably redder. This gives us an indication that the late overall light distribution of SN 1991bg is similar to normal SNIa but for a flux excess in the I band. In Sect. 4.2 this is ascribed to the unusually strong [CaII] emission lines.

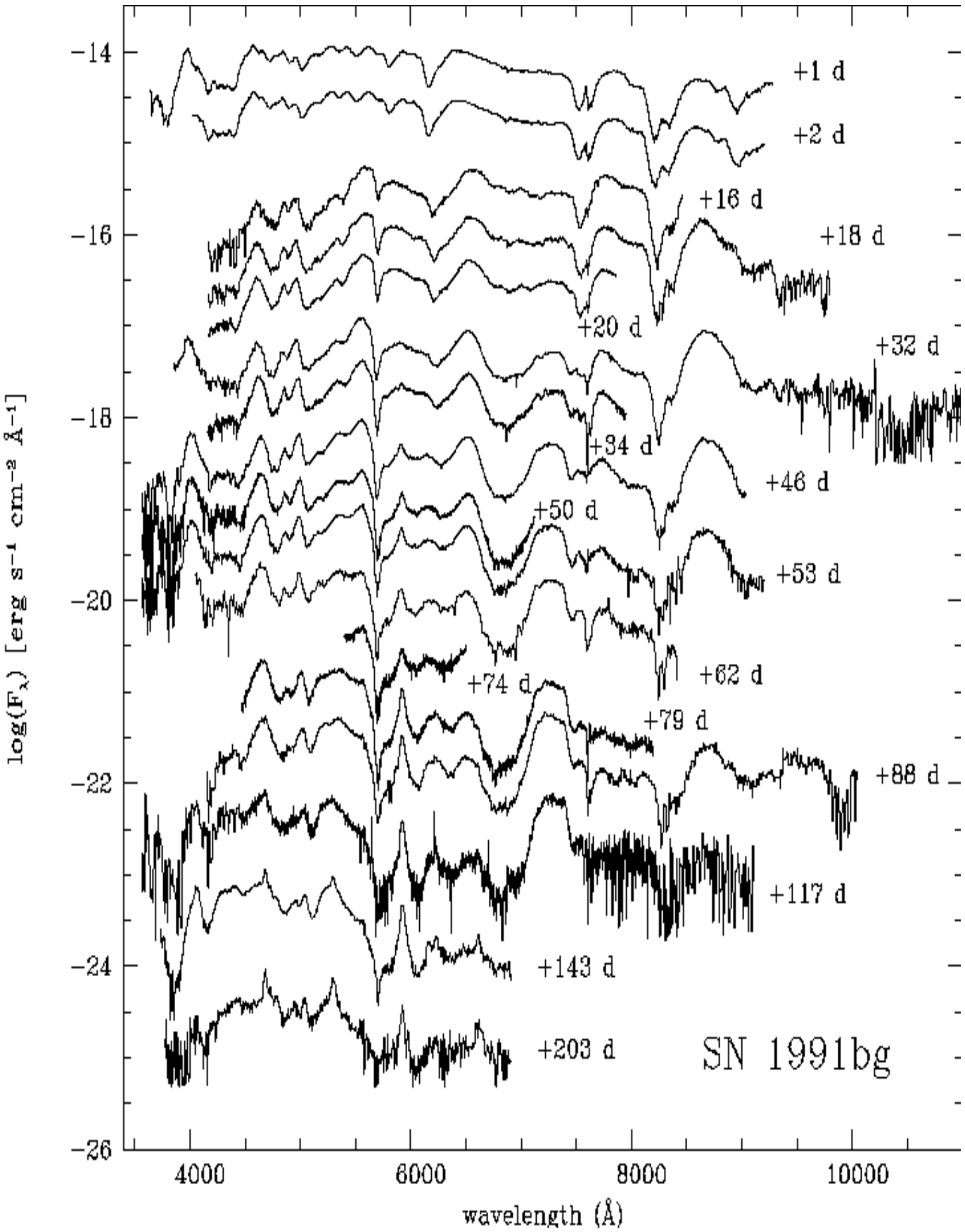

Figure 6. The spectral evolution of SN 1991bg from day +1 to day +203. The ordinate refers to the first spectrum (t=+1 d); all other spectra are shifted downwards by 0.45 dex with respect to the one above, with the exception of the last three, for which the shift is 0.65 dex.

3.4 The bolometric light curve

The optical light curves of SN 1991bg are well defined in four bands for several months. These allowed us to estimate the *uvoir* bolometric luminosity by applying reasonable corrections to the optical data. Suntzeff (1995) showed that in normal SNIa at early phases the flux below 4000 Å is less than 40% of the total flux and rapidly declines below 10% already at 80 days after maximum. Also the contribution of the IR above 9000 Å is always low (less than 15%, Suntzeff (1995)). In the case of SN 1991bg the dominance of the BVRI bands is even larger: merging the (single) IUE spectrum available, taken at B maximum (Cappellaro et al. 1995), with our nearly–simultaneous optical observations, we have estimated that the flux below 4000 Å is only $\sim$ 10% of the total flux in the range 1900–9000 Å. Also the JHK infrared observations of SN 1991bg (Porter et al. 1992) indicate a low luminosity at maximum followed by a rapid decline of 3 mag in the first month, with no sign of a secondary maximum. It is reasonable to assume that in SN 1991bg the UV contribution decreased with epoch while the near-infrared one increased up to 15% of the total *uvoir* flux analogous to SN 1992A (Suntzeff 1995). This means that at all epochs about 80% of the total flux of SN 1991bg is emitted in the BVRI domain, corresponding to a constant correction of 0.10 dex. Spectral modeling, discussed by Mazzali et al. (1996), gives results in good agreement with this assumption.

The evolution of the bolometric luminosity is compared in Fig. 5 to that of SN 1992A (Suntzeff 1995). Both BVRI photometry (from this paper and literature) and spectrophotometric data have been used. A distance modulus of 31.09 and a reddening correction E(B-V)= 0.05 have been adopted (cfr. Sect. 3.2). † Thus SN 1991bg at maximum was about 3 times fainter than the spectroscopically normal SNIa SN 1992A ($logL = 42.65$) and, because of a faster luminosity decline, the difference increased to a factor 5 on day 200. It should be noted that, according to Suntzeff (1995) either the distance scale to SN 1992A is grossly in error, or this type Ia SN is underluminous with respect to the standard model, so the offset in peak L_{Bol} values in Fig. 5 does not indicate that SN 1991bg is a factor 3 fainter than normal SNe Ia.

In Tab. 3 we present the main data of the bolometric light curve. The slopes have been determined making use only of the photometric determinations. It is evident from Fig 5 that SN 1991bg was at all epochs steeper than SN 1992A which declined at a rate of 2.0 $mag \times (100d)^{-1}$ between day 72 and day 210.

At the last epoch of observation (day 530) only the V magnitude is available, and thus no estimate of the bolometric luminosity is possible. We note, however, that assuming at this epoch the same spectral distribution as on day 203, the corresponding *uvoir* bolometric luminosity is about 10^{38} ergs s^{-1}.

† The maximum bolometric luminosity of SN 1991bg, $log_{10}L = 42.20$, is about 0.25 dex (i.e. a factor 1.8 in luminosity) fainter than in Fig. 7 of Suntzeff (1995) who adopted a similar distance modulus and no reddening correction. The inconsistency is probably due to a different correction factor.

4 THE SPECTRAL EVOLUTION

The first available spectra of SN 1991bg were taken near maximum light. Figure 6, which shows the spectra listed in Tab. 2, illustrates the overall spectroscopic evolution from the time of maximum to 7 months later.

4.1 The first two months

Although it showed the distinctive SiII absorption, the first available spectrum, taken at maximum, appeared different from those for typical SNIa. In Fig. 7 the time evolution of the photospheric velocity deduced from SiII λ6355 is plotted. Clearly, the expansion velocity of SN 1991bg was quite low (at maximum, $v_{t=0} = 9720$ km s^{-1}) and declined faster. Also, the blue wing of the SiII doublet, though possibly blended with another weak line, indicates a maximum expansion velocity for the SiII-rich layers of only about 14500 km s^{-1}, to be compared to 16000 km s^{-1} of SN 1994D (Patat et al. 1996).

To highlight the peculiarities of SN 1991bg, in Fig. 8 the spectra of SN 1991bg at different epochs are compared to those of other SNIa at similar phases. Only SNIa with low expansion velocities have been selected. At maximum, the slope of the optical continuum differs from that of the normal SNIa 1994D and 1989B, once the latter is dereddened. Instead, it resembles the slope of SN 1986G (cfr. top panel of Fig. 8) if one adopts for this SN a reddening E(B-V)=0.6 (Phillips 1993). Other similarities with SN 1986G can be seen, in particular in the broad absorption trough between 4200 and 4500 Å which has been early on noted (Benetti et al. 1991). Filippenko et al (1992) attributed this feature to MgII 4481 Å and TiII lines that could also account for a number of other features below 5000 Å, while Leibundgut et al. (1993) identified it with FeIII. The spectrum synthesis analysis (Mazzali et al. 1996) supports the TiII identification.

As in SN 1986G, the red wing of the SiII λ6355Å absorption seems to be contaminated by another absorption line. After deblending, the latter was measured at about 6255 Å in the parent galaxy rest frame. Leibundgut et al. (1993) have proposed CII λ6580 Å or Hα from hydrogen expanding at velocities of the order of 14000 km s^{-1}as possible identifications. The similarity with SN 1986G extends to the absorption at about 5800 Å attributed to SiII λ5968, which in both SNe is stronger than in normal SNe Ia. Also, the two lines of SII near 5500Å have similar intensity, while the redder one is usually stronger in other SNe Ia at this epoch.

As in other SNe Ia spectra, in the near–IR the strong P-Cygni profile of the CaII triplet is possibly contaminated by OI λ8446. The absorptions at 7600 Å, due to OI $\lambda 7772-7775$ and MgII $\lambda 7877-7896$, and that at 8900 Å, due to MgII $\lambda 9217-9243$, are instead much stronger than usual.

There is a two week gap in the temporal coverage both in our spectroscopic observations and in those of Filippenko et al. (1992) and Leibundgut et al. (1993). When the SN was observed again at the end of December, about 2 weeks after maximum, the spectrum was quite different (cfr. Fig. 6). At this point the rapid post-maximum decline phase is over, and the SN enters what, in Sect. 3, we called the *intermediate* phase of the light curve. The continuum is now redder (cfr. also Fig. 4) and emission lines, which are commonly observed

in SNIa only at later epochs, start to appear. The λ6355 SiII absorption is still present, while the corresponding emission has strengthened and has moved redward. [NiIII] λ6536 may also contribute to this emission. On the other hand, the SiII absorption at 5810 Å (5792 Å in the galaxy rest frame) disappeared, probably as a result of the drop in temperature lowering the population of the lower level which is 2 eV higher than the corresponding level giving the SiII 6355 line. The CaII IR lines are very strong and the lines of OI and MgII have decreased their intensities. Now the Ca emission dominates over the absorption.

The strong and relatively narrow absorption feature, measured on day 18 at about 5705 Å (5687 Å in the galaxy rest frame[‡] is quite unusual. This line, which was also barely visible in the spectra at maximum, will persist for about 5 months. The line profile is strongly asymmetric but definitely narrower than all other absorption features in the spectrum, FWHM$\sim$ 2500 km s^{-1}, and constant with time. If the feature is attributed to NaID (Filippenko et al. 1992), the expansion velocity of the absorbing layer, $v_{NaI} = 10500$ km s^{-1}, is much larger than that of SiII ($v_{SiII} = 7600$ km s^{-1}) at this epoch. Leibundgut et al. (1993) attributed this feature at early epochs to a blend of SiII lines but its narrowness with respect to other SiII lines and its persistence after SiII 6355 has faded makes this doubtful. An unlikely identification is HeI λ5876 expanding at about 9600 km s^{-1}, because of the low photospheric temperature, unless non-thermal excitation of appropriate levels is effective. We lack independent evidence of non-thermal effects. In any of these cases, however, the high expansion velocity and the narrow width confine the ion from which the line forms to a relatively thin outer layer. This would then be clear-cut evidence of stratification in SN Ia ejecta.

However the feature changes very little in velocity over the 200 days of observation, in contrast with other absorption features.

The line drifts from 5710 Å on day 1 to 5700 Å at about 50 days past maximum, in good agreement with the measurements of Leibundgut (1993). Thus the correct interpretation may have to await a detailed modeling to ascertain whether radiation transfer effects which describe the redward progression of photons in the expanding photosphere can produce this feature.

On day 50 all absorptions (5700 Å feature excepted) have drifted notably to the red with respect to the initial position, indicating that the photospheric expansion velocity has decreased significantly. The CaII lines appear at early phases stronger in absorption than in other SNIa, in particular the IR triplet; and stronger in emission at later phases, in particular [CaII] λ7291 − 7324. Although abundance effects may play a role, a temperature effect must be important. Apart from this peculiarity, overall the spectrum at this phase resembles that of normal SNIa.

4.2 The nebular phase

For the first time on day 34 we detect a relatively narrow emission line redward of the absorption at 5700 Å, at about 5915 Å (rest wavelength, 5897 Å, cfr. Fig. 6). From this epoch on, and up to our last observation, the relative intensity of this emission keeps increasing. The line profile, with a narrow core, shows very small or negligible velocity evolution redwards. Because of the rest wavelength, the line was identified with the NaID line (Filippenko et al. 1992; Ruiz-Lapuente et al. 1993), but in the light of the results of Mazzali et al. (1996) we propose an alternative identification with [CoIII] λ5890 − 5908, although a contribution from NaID, especially at early phases, cannot be ruled out.

The spectral evolution continues with the progressive decrease of the continuum and the relative increase of the emission lines. The absorptions fade, with the exception of the narrow feature at λ5700. With the third month the SN enters the late decline phase of the light curve (cfr. Sect. 3). Corresponding with this transition the emission line of [CoIII] drifts by about 10 Å to the red, as measured by Leibundgut et al. (1993).

On day 117 the dominant feature is the [CaII] line at 7150-7400 Å (cfr. Fig. 8, bottom) which, as we mentioned, is much stronger than in other SNIa at comparable epoch, while the blue part of the spectrum shows the features typical of other SNIa, although they are significantly narrower. Also, the emissions at 4680 and 5290 Å increase in relative strength as the SN ages.

The last available spectrum of SN 1991bg was obtained on July 3, 1992 (day 203). All lines present on days 117 and 143 are visible and correspond to the typical emission lines in the spectra of SNIa at this epoch (Fig. 9). In particular, the bulk of the emission is between 3800 and 5700 Å, with strong peaks at about 4400, 4700, 5000 and 5300 Å. All lines appears to be significantly narrower than in other SNIa, confirming the indication that the expansion velocity in SN 1991bg was smaller than in typical SNe Ia.

We note that our observations are in contradiction with

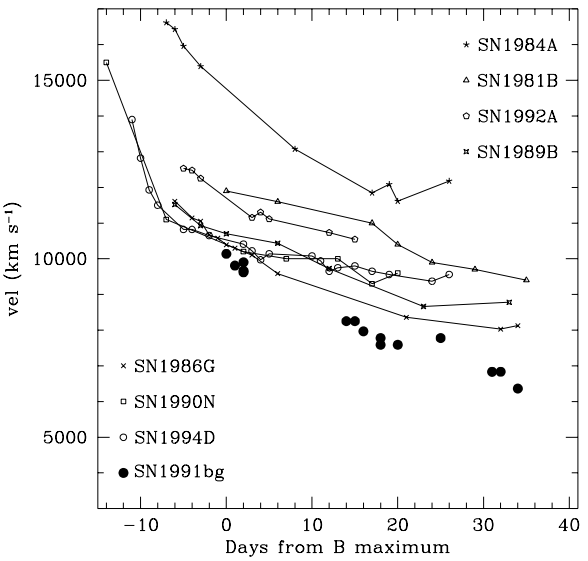

Figure 7. Expansion velocities of SNIa as deduced from the minimum of the SiII λ6355 line. Data of SN 1991bg are from this paper and Leibundgut et al. (1993).

‡ Throughout this paper we have adopted for SN 1991bg the recession velocity of NGC4374, $v = 933$ km s^{-1}(Tully 1988)

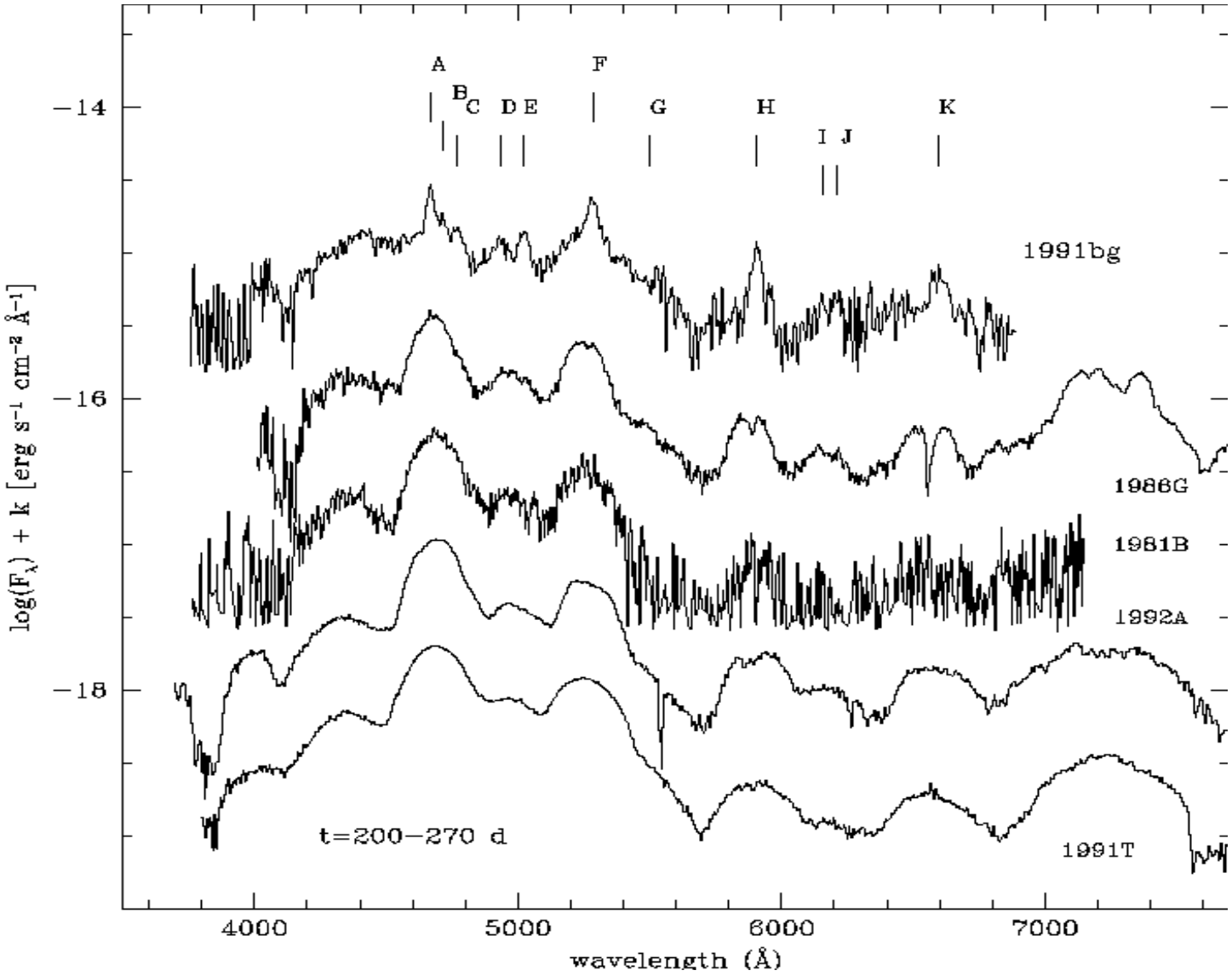

Figure 9. Comparison of the last spectrum of SN 1991bg (203d past maximum) with those of other SNIa at similar epochs: the normal SNe 1981B and 1992A, the peculiar SNe 1986G and 1991T. The spectrum of SN 1986G has been dereddened as in Fig. 8. The narrow emission lines are marked according to Tab. 4. The spectra have been displaced by arbitrary units and reported to the rest frames of the parent galaxies. The spectra of SNe 1981B and 1986G have the same sources as in Fig. 8; the spectrum of SN 1992A has been obtained on Sept. 2, 1992 at the 3.6m telescope equipped with EFOSC; the same equipment was used on Feb. 5, 1992 for SN 1991T.

Table 4. Emissions in the nebular spectra of SN 1991bg

desig.	ident.	rest frame position (Å)			
	epoch:	+88 d	+117 d	+143 d	+203 d
A	[FeIII] 4658-4702		4665	4668	4670
B	[FeIII] 4733			4716	4714
C	[FeIII] 4755-4769-4778			4765	4767
D	[FeIII] 4931		4925	4928	4935
E	[FeIII] 5011		5014	5027	5019
F	[FeII] 5261-5273, [FeIII] 5270		5274	5280	5284
G	[FeII] 5527	5542	5540	5536	5529
H	[CoIII] 5890-5908	5906	5907	5908	5906
I	[CoIII] 6129	6144:		6142	6157
J	[CoIII] 6197	6204	6211	6212	6211
K	[CoIII] 6578, Hα ?	6584	6586	6592	6595

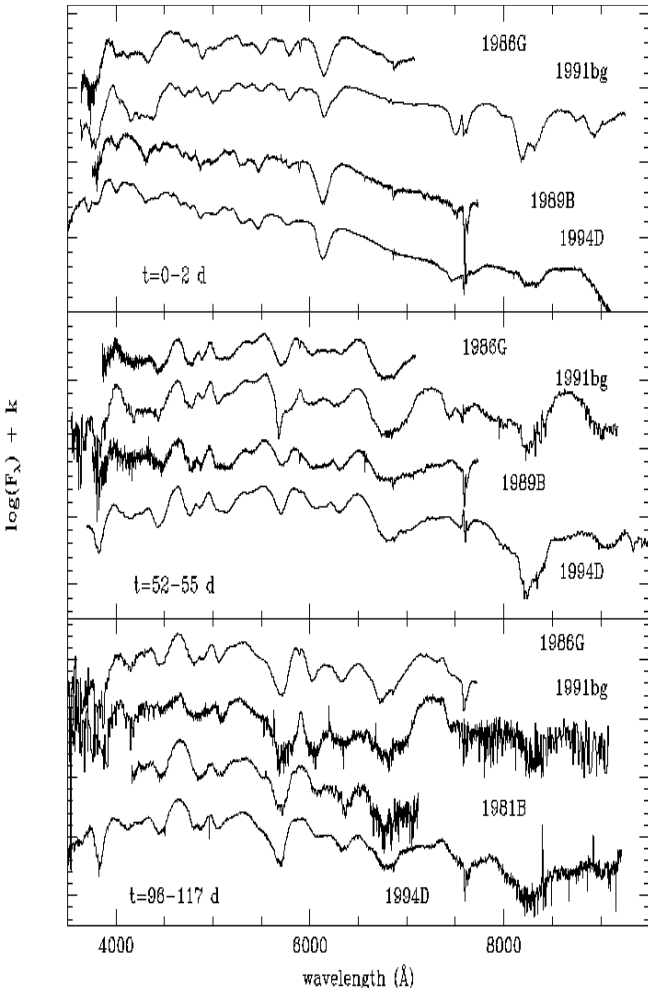

Figure 8. Comparison of the spectra of SN 1991bg at maximum (top panel), around 50 (middle) and 100 (lower) days past maximum with those of other SNIa: the "normal" SNe 1994D and 1981B, 1989B and the peculiar SN 1986G. The spectra of SN 1986G and SN 1989B have been dereddened by E(B-V)=0.6 and 0.35, respectively (Phillips 1993). The tracings have been displaced by arbitrary units and reported to the rest frames of the parent galaxies. References are Cristiani et al. (1992) for SN 1986G; Barbon et al. (1990) for SN 1989B; Patat et al. (1995) for SN 1994D (early times); Branch (1984) for SN 1981B.

those of Ruiz–Lapuente et al. (1993). While their May 24 1992, spectrum resembles our spectrum of May 4, their last spectrum (June 29) taken at the WHT appears remarkably different from our spectra taken only 4 days later. In particular, their spectrum does not show the strong emission features between 4500 and 5500 Å, and is completely different from those of normal SNIa.

A late time spectrum of SN 1991bg, obtained at the same epoch and with the same telescope, was shown by Gomez & Lopez (1995). Although the authors do not state so, this is probably a new reduction of the WHT observation reported by Ruiz–Lapuente et al. (1993). Puzzling enough, the two tracings do not show the same features. In particular, the narrow emissions seen in Ruiz–Lapuente et al. (1993) near 5900 and 6570 Å are absent in the Gomez & Lopez (1995) spectrum, which does not reach wavelengths bluer than 4600 Å. Nevertheless also this spectrum is definitely different from ours.

The most likely explanation for the disagreement between our spectrum and those shown by Ruiz–Lapuente et al. (1993) and Gomez & Lopez (1995) is their inaccurate positioning of the slit on the target and/or a non-alignment of the slit with the parallactic angle. In our case, exploiting the multimode capability of EFOSC, the slit was accurately positioned based on the previous imaging of the field in the B band. An independent confirmation of our spectroscopic calibration is obtained from the $(B-V)$ color curve (Fig. 4) which indicates blue colors for the SN at late epochs.

In Tab. 4 we list the rest frame positions of the narrow lines marked in the late time spectrum of Fig. 9. Typical errors are ± 1 Å but for the features of poorer signal–to–noise ratio for which the errors can be as large as ± 5 Å. Line identifications are based on the NLTE synthetic nebular spectra presented by Mazzali et al. (1996) which reflect the earlier results of Meyerott (1980). The identification of the λ5906 line with [CoIII] is supported both by the line position and by the relative ratio of the flux with the [FeIII] line at about 4700 Å. In fact, according to Kuchner et al. (1994) the time evolution of the Fe/Co flux ratio supports the idea that the Ni–Co–Fe chain powers SNIa. The value of this ratio in our nebular spectra are R= 2.5, 3.0, 4.1 and 4.2 (with errors of the order of 20%) on day 88, 117, 143 and 203, respectively. These values are consistent with those of other SNIa and with the Ni decay model for the origin of Co and Ni also in this SN.

All the other emission features marked in Fig. 9 find satisfactory identifications with forbidden lines of Fe–group elements, with the exception of the feature labeled K, which, on our spectra, is measured at about λ6590Å (rest wavelength) with a FWHM$\sim$ 2000 km s^{-1}, similar to that of the [CoIII] $\lambda 5890-5908$ line. This line is present on all spectra from day 79 onwards, and is also visible in the spectra by Leibundgut et al. (1993) starting at about the same epoch. The line was present in the spectrum of Ruiz–Lapuente et al. (1993) but was measured at λ6570 and identified with Hα. In their proposed scenario, the Hα emission comes from hydrogen stripped from an extended, hydrogen-rich companion star as a consequence of the explosion and it remains at low velocity. Given our measurement of the redshift of this feature of 1200 km s^{-1}with respect to the rest wavelength of Hα, we can exclude the possibility that the line is due to Hα emission from hydrogen surrounding the exploding star. However, we cannot rule out the possibility that the line arises from hydrogen stripped from a companion which at the moment of the explosion was on the far side of the SN with respect to the observer. In this case, high velocity hydrogen blobs mixed with the expanding material might emit redshifted lines. However, since an emission line is present at this wavelength in the nebular spectra of all SNIa (cfr. Fig. 9), and with a width comparable to that of all other spectral features, if this line is attributed to hydrogen in SN 1991bg a similar identification should be invoked for all other SNIa together with the implication that this hydrogen is situated in the expanding envelope. We note that the possibility of interpreting this line as Hα was mentioned by Cristiani et al. (1992) for SN 1986G. Another possible identification is with [CoIII] λ6578, while lines of FeII and [FeII] also fall in this region of the spectrum. Without mod-

eling the identification with [CoIII] is not easy to understand, since it appears to increase in strength relative to the proposed [CoIII] 5890–5908 line. It should be further noted that this feature is slightly redshifted in SN1991bg relative to the broader feature in other supernovae, while there is no significant redward displacement of other emission features at shorter wavelengths. Whether this points to a different identification in this supernova from that in others awaits clarification.

5 ARE THERE RELATIVES OF SN 1991bg ?

In recent years a number of SNe have been indicated as possible relatives (ranging from "twins" to "close cousins") of SN 1991bg.

We already mentioned that SN 1986G was found to share some of the properties of SN 1991bg (cfr Sect. 3.1 & 4), in particular the peculiar broad absorption between 4200 and 4500 Å. Also, the early light curve decline was fast but the duration and the slopes of the various portions of the light curve were different (Leibundgut et al. 1993) and so was the $(B-V)$ color evolution. The absolute magnitude of SN 1986G may have been similar to that of a normal SNIa, but because of the conflicting evidence on the reddening for SN 1986G (cfr. Sect. 5 of Filippenko et al. 1992) no conclusive statement can be made. The late time spectra of SN 1986G showed relatively strong [CaII] lines, similar to SN 1991bg (cfr. Fig. 8, bottom panel), and also the lines were somewhat narrower than in normal SNIa (cfr. Tab. 5) but still broader than in SN 1991bg. It appears, therefore, that while the chemical composition and the physical conditions of the outer layers were rather similar in the two SNe, both showing red continua with TiII lines, at least the kinematics of the inner layers were different.

Filippenko et al. (1992) suggested that SN 1971I is another possible relative of SN 1991bg. Inspection of the light curve shows that this SN, though it faded relatively fast ($12.6\ mag \times (100d)^{-1}$ in B), maintained a close resemblance to typical SNIa until day 300. Moreover, the 4200–4500 Å absorption band is absent in the spectra taken at maximum (Barbon et al. 1973; Kikuchi 1971) and the SiII line indicate a normal expansion velocity (about 11600 km s^{-1} a couple of days before maximum).

In a recent paper by Hamuy et al. (1994) it has been proposed that SN 1992K in ESO 269-G57 is a twin of SN 1991bg. This SN has the broad absorption between 4200 and 4500 Å, a somewhat slow expansion velocity, an intrinsic red continuum and a low luminosity. In Fig. 10 we show the comparison of a spectrum of SN 1992K taken at La Silla on April 7, 1992, with those of SNe 1991bg and 1986G at a similar age. The three spectra are rather similar, both in the blue, with the 4200–4500 Å trough, and in the near IR, with the presence of strong Ca IR triplet and [CaII] $\lambda 7291, 7324$. In SN 1992K, however, the features at 5700 and 5900 Å are broader and similar to SN 1986G.

Although SN 1992K was not observed at maximum, the comparison of the light curves with those of five different templates of SNIa has shown that SN 1992K was indeed very similar to SN 1991bg (Hamuy et al. 1994). In particular, between day 70 and 150, SN 1992K had a decline rate, $\gamma_V = 2.75\ mag \times (100d)^{-1}$, which is identical to that of SN 1991bg (cfr. Tab. 3). Based on this similarity it was possible to estimate that the maximum of SN 1992K occurred probably on Feb. 25, 1992, at an absolute magnitude $M_{\rm B}= -16.84$, slightly brighter (0.4 mag) than 1991bg but still fainter than normal SNIa (we note that also for SN 1992K there is no evidence of significant reddening).

Another SN that has been proposed for inclusion in the SN 1991bg family is SN 1991F in NGC 3458 (Gomez & Lopez 1995). This SN was observed only spectroscopically at epochs estimated between 3 and 5 months past maximum. Similar to SN 1991bg at the same epoch, the spectrum of SN 1991F is dominated by emission lines which are narrower than in normal SNIa, indicating a lower expansion velocity; and it shows strong CaII lines. The presence, in the spectrum taken 80-90 days past maximum, of two very narrow features in absorption at $\lambda 5700$ and in emission at $\lambda 5900$, with profiles very similar to those of the corresponding features in SN 1991bg, is of interest. However, the position of the emission in SN 1991bg (Tab. 4) is about 20-30 Å redder than in SN 1991F (Tab. 2 of Gomez & Lopez 1995) at the same epochs, and, unlike SN 1991bg, the $\lambda 5700$ absorption in SN 1991F weakens with age. Moreover, the [FeII]+[FeIII] emission at about 5200 Å is still weak at t= +144, while in SN 1991bg at the same epoch it is prominent. Rough estimates based on spectrophotometry (Gomez & Lopez 1995) seem to indicate that the late-time luminosity and the decline rate of SN 1991F are comparable to those of SN 1991bg.

In summary, it appears that there are at least three SNIa (namely SNe 1986G, 1991F and 1992K) which share some of the peculiar characteristics of SN 1991bg, in particular the low luminosity, fast fading rate, red colour at maximum, low expansion velocities, evidence of TiII lines in the photospheric spectrum, strong CaII and narrow emission lines at late epochs. However, none of these SNe displayed all these features simultaneously and with such strength as SN 1991bg.

The relative frequency of objects such as 1991bg is difficult to estimate. Because SN searches are magnitude limited, the discovery probability of intrinsically faint SN Ia is lower than that of normal Ia. Therefore, the fraction of faint SN Ia so far discovered (about 5%) must be considered as a lower limit of the true value. On the other hand, the relative rate of faint SN Ia can be estimated based on the few observed events by using the control time method if the details of individual SN searches were known. At present this kind of data is available only for the Asiago+Crimea SN search (Cappellaro et al. 1993). From this database we estimate that faint (1991bg–like) SN Ia are at most 40% of all SN Ia, hence the real number should be between 5 and 40%.

6 DISCUSSION

According to the commonly accepted classification criteria, SN 1991bg was certainly of type Ia. The early spectrum shows most of the typical SN Ia features due to intermediate mass elements, in particular the strong SiII $\lambda 6355$ absorption (Fig. 8), although with noticeable differences in the relative line intensities. This implies that the physical conditions in the near-photospheric layers around maximum light and the outer layers of the exploding star were not dramatically different from the usual ones.

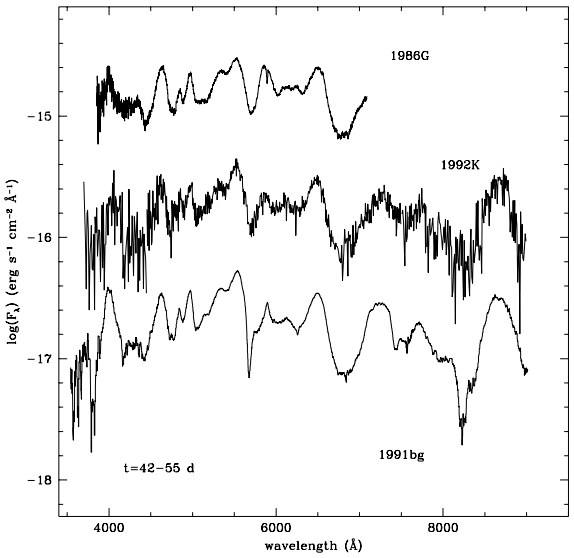

Figure 10. Comparison of the spectrum of SN 1992K taken on April 7 1992 at the 2.2m telescope (with EFOSC2 and grisms n. 1, 5 and 6) and corresponding to an epoch t=+42d (1991bg templates), with those of SN 1991bg on day +46 and SN 1986G on day +55 (Cristiani et al. 1992). The spectrum of SN 1986G has been dereddened as in Fig. 8 and 9. The ordinates are relative to the spectrum of SN 1992K, while the other two have been shifted by arbitrary units for an easier comparison. In abscissa are the rest frame wavelengths.

Contrary to previous claims, we have shown in Sect. 4.2 that also in the nebular spectra of SN 1991bg, in particular in the latest observation at t= 203d (Fig. 9), the relative intensities of the emissions match those of normal SNIa. Since at late epochs the line forming region is deep inside the ejecta, this indicates that the composition as well as the physical conditions of the interior (temperature, density, ionization, etc.) are similar too. However, the lines are significantly narrower, hence the expansion velocity of the ejecta must be smaller. The luminosity at maximum ($M_{\rm B}$= −16.54) is about 2.5 magnitudes fainter than normal SNIa (cfr. Sect. 3.2) while the bolometric luminosity is about 0.5 dex fainter than SN 1992A.

It is believed that the light curve of SNe is powered by the radioactive decay chain ^{56}Ni–^{56}Co–^{56}Fe and that, to a first approximation, the peak (bolometric) luminosity is equal to the instantaneous emission of the radioactive decay (Arnett et al. 1985). As a consequence there is a direct relation between the mass of synthesized ^{56}Ni and the luminosity of the SN: since most SNIa show only a small scatter in absolute magnitude, this implies that most SNIa produce similar amounts of radioactive Ni. At present, explosion models suggest that normal SNIa produce 0.6M$_\odot$ of Ni (e.g. Nomoto et al. (1984).

Therefore if we accept that a normal SNIa produces approximately 0.6 M$_\odot$ of Ni and, from the discussion above, that SN 1991bg had a bolometric luminosity 0.5 dex fainter than SN 1992A, we conclude that SN 1991bg produced < 0.2 M$_\odot$ of Ni (in Sect. 3.4 we noted that SN 1992A might be fainter than normal SNIa). This mass could conceivably be lower still depending on the nature of the explosion and of course on whether SN 1992A produced a smaller mass of Ni. For example Höflich et al. (1995) have demonstrated with a sample of different explosion models that the factor involved in relating bolometric luminosity at maximum to the γ-ray luminosity and hence to mass of Ni could vary by as much as approximately 50 percent. A slightly larger difference in bolometric luminosity between the above two SNe is apparent at 100 days. However an added complication in making a comparative quantitative estimate of Ni mass is the as yet unknown possible difference in γ-ray opacity of the two envelopes also at these later phases.

The mass of ^{56}Ni has been used has an input parameter also in the computation of the late–time synthetic spectra by Mazzali et al. (1996). Consistently low values of M(^{56}Ni) are also suggested in order to reproduce the observed fluxes and line widths in that work.

The rapid luminosity decline of SN 1991bg at early epochs is unique, and is indicative of a small ejecta mass (Filippenko et al. 1992; Leibundgut et al. 1993). If the envelope is small, the diffusion time is short and the trapping of the γ-rays from the radioactive decay of ^{56}Ni is less efficient. Therefore, the envelope cools more rapidly, the photosphere recedes faster in mass coordinates and the luminosity decline is faster.

With the noticeable exception of few peculiar SNe (e.g. SN 1988Z, Turatto et al. (1993b)), the late-time light curve of SNe is powered by the radioactive decay of ^{56}Co into ^{56}Fe, with an e-folding time of 111 days. The decline rate actually observed depends on the fraction of energy deposited. In the massive SNII the envelope is for at least two years optically thick to the hard radiation originating in the decay and the luminosity decline rate, $\sim 1.0\ mag \times (100d)^{-1}$, closely matches the radioactive input. Instead, in SNIa the envelope becomes progressively more transparent to the γ-rays and the observed luminosity decline is steeper than the radioactive energy release. In normal SNIa a decline rate of 1.5 $mag \times (100d)^{-1}$ is observed (Turatto et al. 1990). The very fast decline rate observed in SN 1991bg (2.5 $mag \times (100d)^{-1}$) is probably due to the small envelope mass.

Eventually, the envelope becomes transparent to γ-rays and only the kinetic energy of the positron (about 5% of the total decay energy) is deposited. At this point, the light curve is expected to approach the ^{56}Co decline rate. Indeed, a significant flattening of the light curve is indicated by the last observations of SN 1991bg. The observations available allow only a setting of an upper limit to the late decline rate ($\leq 1.2\ mag \times (100d)^{-1}$). This is consistent with the ^{56}Co input.

Few other SNIa have been observed at phases later than 500 days. One of these was SN 1937C. This SN, although showing a flattening in the photographic light curve around day 300, had a steeper decline rate (1.31 $mag \times (100d)^{-1}$) until day 600 (Schaeffer 1994). The case of SN 1992A is different. For this SN recent HST observations indicate a flattening of the light curve after day 600 to a rate slower than the ^{56}Co decay rate, suggesting additional energy sources such as ^{44}Ti decay, ionization freeze–out or light echoes. In the case of SN 1991T observed at late phases, a light echo began to influence the light curve and caused it to decline considerably slower than would be expected from ^{56}Co de-

cay (Schmidt et al. 1995). This possibility for SN 1991bg cannot be excluded by current observations.

The main spectral peculiarities of SN 1991bg in the photospheric epoch are the low photospheric expansion velocity, the red colour and the presence of the absorption band between 4200 and 4500 Å. It is shown by Mazzali et al. (1996) that these features can be satisfactorily reproduced if the SN is underluminous and if the abundance of the Fe–group elements above 3500 km $s^{-1}$is low compared to the standard W7 model. An overabundance of Ti with respect to other intermediate mass elements is not required in order to explain the λ4200–4500 feature, which is the result of the low ionization due to the low luminosity.

The peculiarities of the late time spectra of SN 1991bg with respect to other SNIa are highlighted in Fig. 9. The SNe are plotted from top to bottom in sequence of increasing line widths. It is interesting to note that the objects define also a sequence of absolute magnitudes. In Table 5 we list the absolute magnitudes at maximum, the value of Δm_{15}(B), the photospheric velocity at maximum as derived from the SiII line (which may be an overestimate of the actual value, cfr. Patat et al 1995), and the FWHM of the [CoIII] lines in the late time spectra between day 200 and 270. The [CoIII] line has been measured because it may be less affected by blending than other lines, e.g. [FeII] and [FeIII], but the same trend holds also for other emission lines in the nebular spectrum.

A relation between the peak luminosity and the rate of decline, with faster fading SNIa being fainter, was first suggested by Pskovskii (1967) and has recently been confirmed on the basis of accurate CCD photometry (Phillips 1993; Hamuy et al. 1995). The trend is well illustrated by the SNe in Table 5, which are a subsample of those of Phillips (1993). From Table 5 we also note that the correlation extends also to the photospheric expansion velocities at maximum and to the expansion velocities of the innermost layers as deduced from the line widths of the Fe-peak elements. The very small velocity in SN 1991bg suggests that in this SN complete nuclear burning was confined to the innermost regions. In other words, observations indicate that SNIa with more slowly expanding ejecta, in particular SN 1991bg, have a more rapid photometric evolution and reach a fainter absolute magnitude than fast expanding objects.

Arnett (1982) has shown how the ^{56}Ni mass is directly proportional to the square of the velocity scale of expansion. Both the low photosphere and nebular velocities therefore point directly to a low mass of Ni produced in SN 1991bg. Nevertheless the quantification of this finding is beset by difficulties in defining observationally which velocity should be used. At early phases, because of the great strength of the SiII line, a photospheric velocity is not well defined, while at the late phases the velocities from the widths of the emission lines refer to material concentrated in the innermost parts of the exploding star.

A number of possible explosion scenarios have been proposed to explain the peculiar characteristics of SN 1991bg, and in general the faint SNIa.

Hoflich et al. (1995) used Delayed Detonation models to explain SNIa light curves. They argued that, depending on the density at which the transition from deflagration to detonation occurs, different ^{56}Ni masses and, therefore, SNIa of different luminosity can be produced by the same explosion mechanism in a Chandrasekhar mass C-O WD. In particular, their PDD5 model, which produces 0.12 $M_\odot$ of ^{56}Ni, gives the best fit to the SN 1991bg observations. In this model the ^{56}Ni is strongly concentrated in the center, as indicated also by our observations, and a major fraction of the mass is in intermediate mass elements, with only about 0.05 $M_\odot$ of unburned C/O left after the explosion. However, this model requires a large reddening, E(B-V)=0.30, in order to reconcile the predicted luminosity with the observed value, while observations indicate a much smaller value, E(B-V)= 0.05 (cfr. Sect. 3.2). Also, the decline rates of the PDD5 model are similar to those of their standard Ia model (N32), while we found SN 1991bg to be faster (cfr. Sect. 3).

An alternative scenario for faint SNIa was proposed by Livne (1990) and Woosley & Weaver (1994). In their models a C–O white dwarf with mass below the Chandrasekhar limit accretes He at a rate of the order of a few 10^{-8} $M_\odot$ yr^{-1} until He ignites at the bottom of the layer. The in-going shock wave induces a detonation of the C-O which disrupts the star. According to Woosley & Weaver (1994) less massive white dwarfs produce smaller ^{56}Ni masses and less energy, in qualitative agreement with our findings. The lower mass WD results in a larger fraction of intermediate mass elements and an overproduction of other isotopes (including Ti^{44}) in the He detonation layer, while a large fraction of He is left unburned. We already noted, however, that an overproduction of ^{44}Ti is not required by the spectral synthesis models. The visibility of He in the ejecta is not expected because of the observed low temperatures. Moreover, the models of Mazzali et al. (1996) seem to exclude the short rise times to maximum light (of the order of 13d) which are obtained by Woosley & Weaver (1994). These sub–Chandrasekhar models produce in the interior a nearly constant velocity as a function of mass and, therefore, they do not the reproduce the low velocities observed in SN 1991bg at late stages.

In another explosion mechanism, proposed by Nomoto et al. (1995), a low mass of ^{56}Ni is produced by the collapse of a O–Ne–Mg WD formed after the merging of a double C–O WD system. In order to reproduce the observed luminosity the collapsing core has to be embedded in a C–O envelope of 0.6 $M_\odot$ and the shock wave propagating through it produces 0.15 $M_\odot$ of ^{56}Ni, compatible with the estimates

Table 5. Expansion velocities vs. absolute magnitude for SNIa

SN	M_V^{max}	$\Delta m_{15}(B)$	v(SiII)[a] [km s^{-1}]	FWHM([CoIII])[b] [km s^{-1}][day]
1991bg	-17.28	1.95	9800	2340 [203]
1986G	-18.22[c]	1.73	10400	7120 [256]
1981B	-18.50	1.10	11900	8140: [270]
1992A	-18.00	1.33	11700	10170 [227]
1991T	-19.51[d]	0.94	9800[e]	11190 [262]

(a) photospheric velocity at B maximum as measured from the SiII λ6355 absorption; (b) Full Width Half Maximum of [CoIII] λ5890 − 5908 emission at epochs between 200 and 270 days (indicated in brackets); (c) E(B-V)= 0.6 (Phillips 1993); (d) E(B-V)= 0.13 (Phillips et al. 1992); (e) the expansion velocity of SiII in SN 1991T was a poor indicator of the photospheric velocity. Velocities measured from other lines were significantly larger than in normal SNIa (Phillips et al. 1992).

found above. The resulting light curve reproduces satisfactorily the observed one in the early 100 days but Si seems to be located at velocities too high to reproduce the observed lines.

Unfortunately the observations alone do not suggest unambiguously a preferred model for the progenitor. All suffer from the various difficulties discussed above. Mazzali et al. (1996) show through modelling that even in the most promising models one has to resort to ad hoc adjustments of abundances and their stratification to approximate the observed spectra. Thus SN 1991bg has provided an additional challenge to our understanding the Type Ia supernova phenomena.

7 CONCLUSIONS

The new observations presented in this paper confirm the peculiar characteristics of SN 1991bg and give new insights into its late time behaviour.

In particular, SN 1991bg was fainter than normal SNIa by about 2.5 magnitudes in the B band, but by less than 2 mags in the V band, thus giving a particularly red colour at maximum, $(B\text{-}V)_{max} = 0.74$. However, because of a different colour evolution, the SN turned to the colour curve of normal SNIa already 40–50 days later. The rates of decline in all optical bands (BVRI) are at all epochs the most rapid ever observed in SNIa (Tab. 3). The constructed *uvoir* bolometric light curve is consequently steeper than in the normal SN Ia SN 1992A. A very deep V band observation obtained 530 days past maximum showed that before this epoch the fading rate had decreased to about $1.2\ mag \times (100d)^{-1}$, and we stress that, on the basis of the available data, energy sources other than Co decay are not required.

The low luminosity at maximum is an indication that the SN produced a small mass of Ni ($< 0.2\ M_{\odot}$), whereas the fast photometric evolution was related to a small mass of the envelope. The small explosion energy also causes the photosphere at maximum light to be cooler than in typical SNIa, as is evident when comparing the early time spectra. This also explains the broad absorption feature between 4200-4500 Å identified with TiII, which has been attributed to an ionization effect by Mazzali et al. (1996).

A peculiarity of the spectrum of SN 1991bg at epochs subsequent to maximum is the presence of the two narrow features at about 5700Å (in absorption) and 5900Å (in emission). The absorption lacks at the moment a convincing explanation mainly because there is no significant evolution redwards, while the emission, which appeared already on day 34, is plausibly an early emergence of [CoIII] in accordance with the fast evolution to the nebular stage shown by SN 1991bg. It has been noted that the spectrum of SN 1991bg evolved to the nebular stage earlier than usual.

Contrary to previous claims, the overall appearance of the spectrum maintained a general resemblance to those of other SNIa at least until 200 days after maximum light (Fig. 9), indicating that the ionization conditions of the Fe core were similar to those of other SNIa at this phase. In particular, there has been no sudden change in the nature of the spectrum during the interval day 143 to day 203. Nevertheless, the emission lines were exceptionally narrow, and allowed the identification of the main emissions with lines of [FeII], [FeIII] and [CoIII]. The presence of hydrogen at late times seems unlikely.

The small photospheric expansion velocity and envelope mass, combined with the the small expansion velocity and mass of the Fe–group core, as seen from the late-time spectra and luminosity, point to a kinetic energy smaller than in typical SNIa. We pointed out that the correlation between the luminosity at maximum and the early rate of decline can be extended also to the expansion velocities of the photosphere at maximum and to the innermost layers emitting the nebular spectrum (Tab. 5). In other words, the luminosity at maximum correlates to the kinetic energy of the SNIa.

One important question is whether the lower energy SN 1991bg can be considered an extreme case of a continuous distribution of SNIa or whether it is a representative of a separate subclass of faint SNe Ia. We reviewed the literature and found that while a handful of other SNIa shared some of the observed characteristics of SN 1991bg, none was quite so extreme. This may support the concept of a continuum transition from faint SNIa (SN 1991bg–like) to *normal* ones. Obviously, a continuum of SN Ia properties might jeopardize their use as standard candles, at least until one understands better the inter-relation between light curves and spectral characteristics.

ACKNOWLEDGMENTS We thank Roberto Rampazzo and Caterina Zanin for obtaining some of the observations reported in this paper.

This work has been conducted as part of the ESO Key Programme on Supernovae

REFERENCES

Arnett, W.D., 1982, in "Supernovae: A Survey of Current Research", D. Reidel: Dordrecht, Holland, p. 221
Arnett,W.D., Branch,D., Wheeler,J.C., 1985, Nature 314 337
Barbon,R., Ciatti,F., Rosino,L., 1973, A&A 25, 241
Barbon,R., Ciatti,F., Rosino,L., 1973, Mem.S.A.It. 44, 65
Barbon,R., Benetti,S., Cappellaro,E., Rosino,L., Turatto,M., 1990, A&A 237, 79
Benetti,S., Cappellaro,E., Turatto,M., 1991, IAUC 5405
Branch,D., 1984, in Evans D.S., ed., XI Texas Symposium on Relativistic Astrophysics, N.Y. Academy of Science, 422, 186
Branch,D., 1992, ApJ 392, 35
Burstein,D., Heiles,C., 1984, ApJS 54, 33
Cappellaro, E., Turatto, M., Benetti, S., Tsvetkov, D.Yu., Bartunov, O.S., Makarova, I.N., 1993, A&A 273, 383
Cappellaro,E., Turatto,M., Fernley,J., 1995, Supernovae, IUE – ULDA Access Guide N.6, ESA SP-1189, Noordwijk
Ciardullo,R., Jacoby,G.H., Tonry,J.L., 1993, ApJ 419, 479
Cristiani,S., Cappellaro E., Turatto M., Bergeron,J., Bues,I., Buson,L.M., Danziger,I.J., Di Serego Alighieri,S., Duerbeck,H.W., Heydari-Malayeri,M., Schmutz,W., Schulte-Ladbeck,R.E., 1992. A&A 259, 63
Filippenko,A.V., Richmond,M.W., Branch,D. Gaskel,C.M., Herbst,W., Ford,C.H., Treffers,R.R., Matheson,T., Ho,L.C., Dey,A., Sargent,W.L.W., Small,T.A., Bruegel,W.J.M., 1992, AJ 104, 1543.
Frogel,J.A., Gregory,B., Kawara,K., Phillips,M.M., Laney,D., 1987, ApJ 315, L129
Gomez,G., Lopez,R., 1995, AJ 109, 737
Hamuy,M., Phillips,M.M., Maza,J. Suntzeff,N.B., Della Valle,M., Danziger,I.J., Antezana,R., Wischnjwesky,M., Aviles,R., Schommer,R.A., Kim,Y.C., Wells,L.A.,

Ruiz,M.T., Prosser,C.F., Krzeminski,W., Baylin,C.D., Hartigan,P., Hughes,J., 1994, AJ 108, 2226
Hamuy,M., Phillips,M.M., Maza,J., Suntzeff,N.B., Schommer,R.A., Aviles,R., 1995, AJ 109, 1
Hoflich,P., Khokhlov,A.M., Wheeler,J.C., 1995, ApJ 444, 831
Hoflich,P., Khokhlov,A.M., 1996, ApJ 457, 500
Kikuchi,S., 1971, PASJ 23, 593
Kosai,H, Kushida,R., Kushida,H., Kato,T., 1991, IAUC 5400
Kuchner,M.J., Kirshner,R.P., Pinto,P.A., Leibundgut,B., 1994, ApJ 426, L89
Landolt A.U., 1992, AJ 104, 340
Leibundgut,B., Kirshner,R., Phillips,M.M., et al., 1993, AJ 105, 301
Livne,E., 1990, ApJ 354, L53
Maza,J., Hamuy,M., Phillips,M.M., Suntzeff,N., Aviles,R., 1994, ApJ 424, L107
Mazzali P.A., Danziger,I.J., Turatto,M., 1995, A&A 297, 509
Mazzali P.A., Chugai, N., Turatto, M., Lucy, L., Danziger, I.J., Cappellaro, E., Della Valle, M., Benetti, S.., 1996, MNRAS submitted
Meyerott, R.E., 1980, ApJ 239, 257
Nomoto,K., Thielemann, F.K., Yokoi, K., 1984, ApJ 286, 644
Nomoto,K., Yamaoka,H., Shigeyama,T., Iwamoto,K., 1995, in McCray,R. & Wang,Z., ed., Supernova and Supernova Remnants, Cambridge University press, Cambridge, in press
Patat,F., Benetti,S., Cappellaro,E., Danziger,I.J., Della Valle,M., Mazzali,P., Turatto,M., 1996, MNRAS 278, 111
Porter,A.C., Dickinson,M., Stanford,S.A., Lada,E.A., Fuller,G.A., 1992, BAAS 24, 1244
Phillips,M.M., Well,L.A., Suntzeff,N.B., Hamuy,M., Leibundgut,B., Kirshner,R.P., Foltz,C.B., 1992, AJ 103, 1632
Phillips,M.M., 1993, ApJ 413, L105
Pskovskii,Y.P., 1967, SA 11, 63
Pskovskii,Y.P., 1971, SA 14, 798
Ruiz-Lapuente,P., Cappellaro,E., Turatto,M., Gouiffes,C., Danziger,I.J., Della Valle,M., Lucy,L.B., 1992, ApJ 387, L33
Ruiz-Lapuente,P., Jeffery,D.J., Challis,P.M., Filippenko,A.V., Kirshner,R.P., Ho,L.C., Schmidt,B.P., Sanchez,F., Canal,R., 1993, Nature 365, 728
Saha,A., Sandage,A., Labhardt,L., Schwengeler,H., Tammann,G.A., Panagia,N., Macchetto,F.D., 1995, Ap. J. 438, 8
Sandage,A., Tammann,G.A., 1993, ApJ 415, 1
Schaeffer,B.E., 1994, ApJ 426, 493
Schmidt,B.P., Kirshner,R.P., Leibundgut,B., Wells,L.A., Porter,A.C., Ruiz–Lapuente,P., Challis,P., Filippenko,A.V., 1995, ApJ 434, L19
Suntzeff,N.B., 1995, in McCray,R. & Wang,Z., ed., Supernova and Supernova Remnants, Cambridge University press, Cambridge, in press
Tully, R.B., 1988, Nearby Galaxy Catalog, Cambridge University Press, Cambridge
Turatto M., Cappellaro E., Barbon R., Della Valle M., Ortolani S., Rosino L., 1990, AJ, 100, 771
Turatto M., Cappellaro E., Benetti,S., Danziger I.J., 1993, MNRAS, 265, 471
Turatto M., Cappellaro E., Danziger I.J., Benetti,S., Gouiffes, C., Della Valle,M., 1993, MNRAS, 262, 128
Turatto M., Cappellaro E., Benetti,S., 1994, AJ 108, 202
Vaughan,T.E., Branch,D., Miller,L., Perlmutter,S., 1995, ApJ 439, 558
Weaver,T.A., Axelrod,T.S., Woosley,S.E., in Wheeler,J.C., ed., Proc. Workshop on Type I Supernovae, University of Texas, Austin, p.113
Wheeler,J.C., Benetti,S., 1995, Astrophysical Quantities, IVth edition, ed. Arthur N. Cox, in press
Woosley,S.E., Weaver,T.A., 1994, ApJ 423, 371

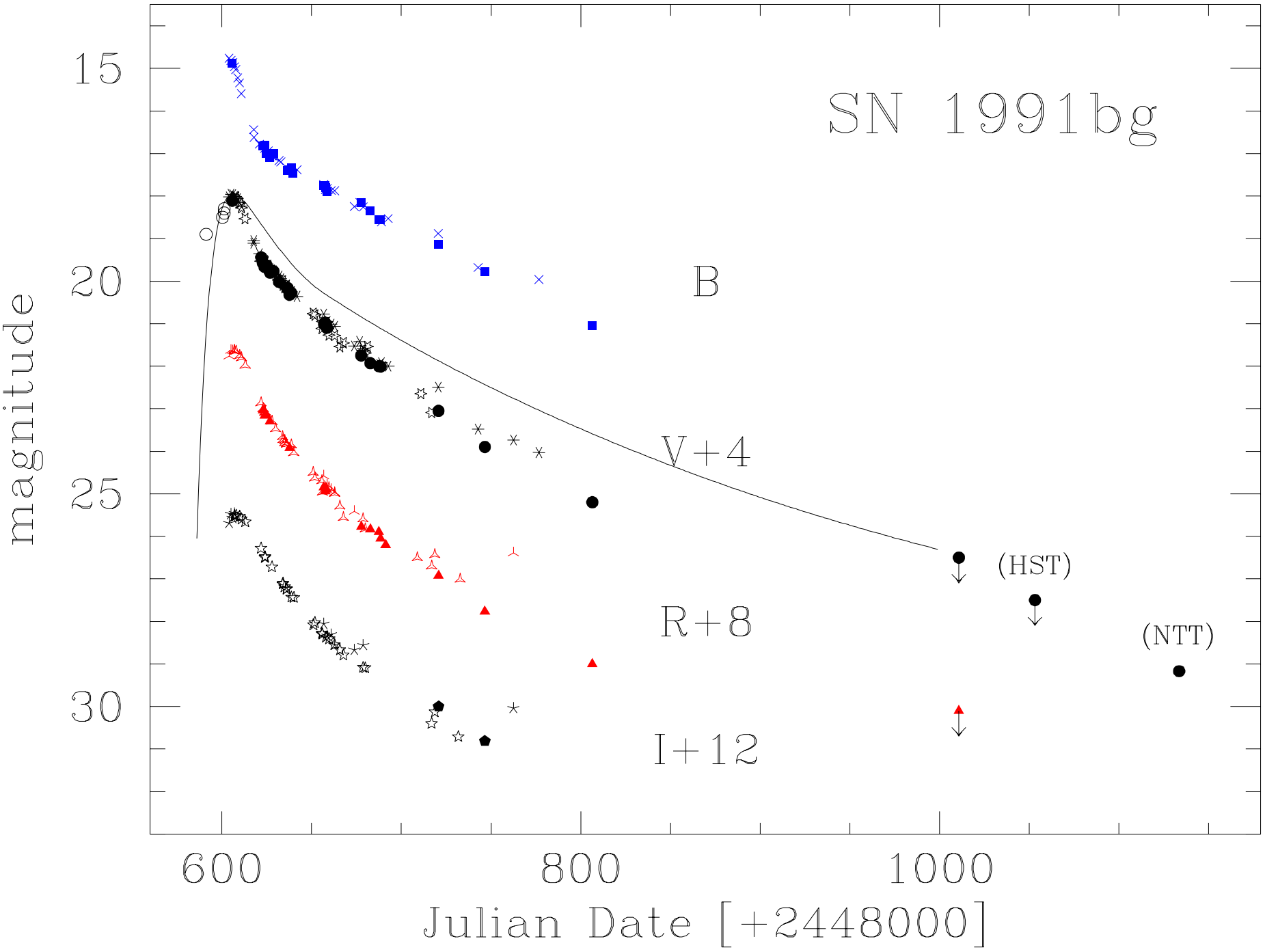
SN 1991bg
B
V+4
R+8
I+12
(HST)
(NTT)
magnitude
15
20
25
30
600
800
1000
Julian Date [+2448000]